Spectrophotometric Analysis of Nano Ca-Bentonite Tactoid Breakdown by Exchangeable Na+ and K+

Ahmed R. Ghoniemy, El Adly, R. M and Adel M. Elprince
Soils and Agricultural Chemistry Dept., Faculty of Agriculture, Alexandria University , Egypt

DOI: 10.21608/ajsws.2024.284561.1015

Article Information

Received:April 22 2024

Revised:April 28 2023

Accepted:April 30 2024

Published:Semptemer 1 2024

ABSTRACT: The montmorillonite mineral, commonly found in soil clay fractions, forms Ca-tactoids, composed of stacked platelets. Interactions between cations in the soil solution, such as Na+ and K+, and Ca-tactoids through ion-exchange processes can lead to the breakdown of these structures into single platelets, thereby influencing soil properties. Previous studies have employed spectrophotometry to measure properties of montmorillonite suspensions, investigating phenomena such as light transmission and scattering. However, challenges exist in applying these methods accurately, particularly concerning variations in adsorbed ion composition and particle-size range. This study aims to address these challenges and advance understanding by (i) developing a theoretical framework for spectrophotometry that enhances sensitivity to particle dimensions, (ii) analyzing logistic function parameters to gain insights into platelet growth, and (iii) investigating the effects of suspension ageing on tactoid aggregation. XRD and TEM results indicated that a nano Na-bentonite after removal of impurities held four clay minerals: smectite (most probably montmorillonite), kaolinite, illite, and palygoreskite. This nano Na-bentonite used to prepare nano NaB-CaB salt free suspensions having charge fractions of exchangeable sodium, NNa equal 0, 0.1, 0.2,…, 1.0. A similar set was prepared for nano KB-CaB suspensions. Results demonstrated that smectite tactoids saturated with Ca2+ undergo partial breakdown by exchangeable Na+ up to a charge fraction of 0.5, resulting in a steeper increase in light transmittance and decline in absorbance at 800 nm wavelength compared to 700 and 550 nm. Complete breakdown of Ca tactoids occurred at charge fractions above 0.8. Conversely, exchangeable K+ acts as a staking agent up to a charge fraction of 0.5, leading to slower platelet growth compared to Na+. Monte Carlo simulations revealed distinct binding behavior of Na+ and K+ ions on the bentonite surface. Furthermore, the study highlighted the higher efficacy of K+ over Na+ in replacing exchangeable Ca2+, attributed to differences in hydrated ion radius and standard free energy values. Overall, these findings contributed to a deeper understanding of the ion-induced delamination dynamics in bentonite. Furthermore, the study examined the impact of ageing on tactoid dynamics in nano NaB-CaB and KB-CaB suspensions over 7, 61, and 93 days. Spectrophotometry absorbance data, measured at 800 nm wavelength, revealed distinct differences in the single platelet growth rates (parameter c of the logistic function) between NaB-CaB and KB-CaB suspensions, with NaB-CaB exhibiting higher c values across all ageing periods. Specifically, exchangeable Na+ was 34% more effective than exchangeable K+ in breaking down Ca-tactoids. The present study demonstrates that spectrophotometry with sound theoretical bases, carefully prepared suspensions, and logistic modelling, was a useful technique to characterize clay dispersion, particularly in aggregated systems.

Keywords: Tactoid and quasicrystal, *NNa mole charge fraction of exchangeable Na+, Ca-Smectite tactoid, X-ray diffractogram, TEM transmission electron microscopy, logistic function parameters a, b, c, and d, Monte Carlo simulations, ion-exchange standard free energy, tactoid ageing.*

INTRODUCTION

Interactions between cations in the soil solution, such as Na^+ and K^+, and Ca-quasicrystals through ion-exchange processes can lead to the breakdown of these structures into single platelets, thereby influencing soil properties. The terminology used to describe these structures, particularly the debate between "tactoid" and "quasicrystal," is significant. While "quasicrystal" has been utilized by soil scientists since the recommendation by Aylmore and Quirk (1971), it is essential to note that in material science, "quasicrystal" refers to materials distinct from smectite clay. Clay minerals, including smectite, typically have regular crystal structure based on repeating unit cells that show lattice translational and rotational symmetry (Kittle, 1953). Quasicrystals, on the other hand, have a non-repetitive pattern and have rotational symmetry without translational symmetry (Enrique Maciá-Barber, 2020). For clarity, we adopt the term "tactoid" analogous to the term "crystallite" used by crystallographers (Waseda et al., 2011).

Tactoids represent the fundamental units of smectite minerals, including montmorillonite, beidellite, and nontronite in the dioctahedral series, and hectorite and saponite in the trioctahedral series (Mering, 1975 and Sposito, 1984). These units consist of hydrated elementary layers (platelets) stacked along the crystallographic c axis, with the number of stacked platelets determined by the types of exchangeable cations present. The measurement of the absorbance of light scattering leads to estimating the number of platelets per tactoid in suspensions of montmorillonite having different single exchangeable cation (Banin and Lahav, 1969). This is done with the convention that Li-montmorillonite suspensions have only single-platelet tactoid. Figure 2 in Banin and Lehav (1969) shows the absorbance ratio A_i/A_{Li} versus the relative number (n) of platelets per tactoid for exchangeable cations (assuming n = 1 for Li-montmorillonite). We fitted these data to the power function $n_i = 0.99\ (A_i/A_{Li})^{1.2531}$ which yields n_i equal to 1, 1.2, 1.6, 2.2, 3.8, 8.4, 9.3, and 9.7 for Li, Na, K, NH_4, Cs, Mg, Ca, and Ba, respectively.

Sheinberg and Otoh (1968) show how the light transmission of montmorillonite suspensions depends on the equivalent fraction of exchangeable sodium in the adsorbed phase where the complementary ion is calcium. Furthermore, Sheinberg and Kaiserman (1969) studied the kinetics of this ion exchange process, namely the transformation of the Ca-montmorillonite tactoids to single platelets of the Na-montmorillonite. The mixing together of Na- and Ca montmorillonite suspensions to produce an overall charge fraction of Na^+ on the clay particles below 0.1 results in a very rapid (less than 1 min) formation of quasicrystals from conversion of the Na-montmorillonite particles. However, Keren and Klein (1995) indicate that spectrophotometry should consider the limitations of light transmission and scattering theories. A critical review of research papers on the montmorillonite-quasicrystals (tactoids) is done by Sposito (Sposito, 1984).

Previous studies have employed techniques like spectrophotometry to measure properties of montmorillonite suspensions, investigating phenomena such as light transmission and scattering. However, challenges exist in applying these methods accurately, particularly concerning variations in adsorbed ion composition and particle-size range. This study aims to address these challenges and advance understanding by (i) developing a theoretical framework for spectrophotometry that enhances sensitivity to particle dimensions, (ii) analyzing logistic function parameters to gain insights into platelet growth, and (iii) investigating the effects of suspension ageing on tactoid aggregation.

THEORETICAL

Overall, this “THEORETICAL” part provides a through explanation of the principle underlying spectrophotometry analysis of nano suspensions, including light scattering and absorption phenomena, as well as the application of logistic functions for data interpretation. It sets a strong theoretical framework for the subsequent experimental analysis described in the manuscript.

Light scattering and absorption phenomena

The measurement of light scattering from particles is a key analysis tool that provides information on the size, shape, and molecular weight of the particles. Rayleigh scattering and the more general Mie solution are the two best known theories for elastic scattering (Sorensen, 2003; Moore and Cerasoli, 2010). This section provides a theoretical foundation for spectrometry analysis of nano suspensions.

Scattering, Absorption, and Extinction Nomenclature

I_{trans} = the intensity of the light transmitted (not scattered) after passing a distance x through the medium.
I_o = the intensity of the incident light.
τ = the turbidity of the medium.
c = number of particles per unit volume.
σ_{ext} = particle extinction cross section.
σ_{abs} = particle absorption cross section.
σ_{scat} = particle scattering cross section.
β = the size parameter = $2 \pi a / \lambda$
a = Spherical particle radius.
λ = wavelength of the incident light.
Q_{scat} = scattering efficiency.
F(m) = Lorenz term, a function of refractive index term.
E(m) = Lorenz term, a function of refractive index imaginary part.
V = particle volume.
α = means proportional to.

When light passes through a medium containing particles, it is attenuated. This attenuation is called extinction and is described by an exponential decrease of the intensity as it passes through the medium:

$$I_{trans} = I_0 e^{-\tau x}$$

where I_{trans} is the intensity of the light transmitted after passing a distance x through the medium, and τ is the turbidity of the medium. The turbidity is related to the number density of particles n and their individual extinction cross section σ_{ext} by

$\tau = n \sigma_{ext}$

Extinction is due to both scattering, which removes light from the incident path, and absorption, which converts the light into other forms of energy (e.g., heat),

$\sigma_{ext} = \sigma_{abs} + \sigma_{scat}$

These facts are true for particles of all sizes, not just Rayleigh scatterers. From the discussion above two notable features arise:

1. If m is real, extinction is solely due to scattering

$\sigma_{ext} = \sigma_{scat}$

2. If m is complex and if the size parameter is small, $\alpha < 1$, e.g., Rayleigh scatterers, then Equations 14.13 and 14.15 imply $\sigma_{abs} >> \sigma_{scat}$. Hence

$\sigma_{ext} = \sigma_{abs}$

Sorensen (2003) shows that the scattering efficiency, is:

$Q_{scat} = (8/3)\ \beta^4\ F(m)$ (1)

And the absorption efficiency, is:

$Q_{abs} = -4\ \beta\ F(m)$ (2)

Note that the condition for Rayleigh scattering to hold is $\beta << 1$; thus Eq. 1 implies that Rayleigh scatterers are not very efficient, i.e., it scatters a lot less than its geometric cross section would imply.

$\sigma_{scat}\ \alpha\ \lambda^{-4}\ V^2$

$\sigma_{abs}\ \alpha\ \lambda^{-1}\ V$

Equations (1) and (2) imply.

$\sigma_{abs} >> \sigma_{scat}$ Hence,

$\sigma_{ext} \sim= \sigma_{abs} = cons.\ \lambda^{-1}\ V$

$Abs = \log (I_o/ I) = 0.4343\ \tau$

$Abs = cons\ c\ \lambda^{-1}\ V$

Thus, the nanoparticles diameter << λ allows a large fraction of the scattered light (photons) to leave the cuvette in same direction of the incident light. This result agrees with (Sposito, 1984 page 203) that the intensity of light transmitted (not scattered) by a suspension, its constituent particles expected to be directly sensitive to particle dimensions.

Fitting Spectrophotometric Data to a Logistic Function

The logistic function's characteristic S-shaped curve and its parameters provide insights into the growth, saturation, or adoption behavior of the system under consideration. For suspensions of Na-B-CaB, going from $N_{Na} = 0$ to 1, means going from CaB to NaB which is a process of delamination (exfoliation). The logistic model was utilized to model the growth of the delaminated platelets as N_{Na} increased from 0 to 1. The light absorbance and transmittance data for NaB-CaB suspensions were fitted to the logistic function:

$$\text{Abs or T} = \left(\frac{a-d}{1+\exp[-c\ (x-b)]}\right) + d \qquad (3)$$

Abs is absorbance, T is transmittance, and a, b, c, and d are parameters that describe the shape of the curve. Specifically, a and d are the minimum and maximum asymptotes of the curve, respectively. b is the inflection point, which is the value of x at which the curve changes from concave to convex. Finally, c is the slope of the curve at the inflection point.

The c value is a measure of how steeply the curve changes at the inflection point. A larger value of c indicates a steeper curve, while a smaller value of c indicates a more gradual curve around the inflection point b. The derivative of the logistic function is:

$c = f(x) * (1 - f(x))$ (4)

Therefore, the slope of the curve at the inflection point b is $c = f(b) * (1 - f(b))$. The statistical error was computed using the Root Mean Square Error (RMSE) method, which measures the average deviation between predicted (Y) and actual y(x) values. The formula for RMSE is:

$RMSE = sqrt\ [(1/n) * \Sigma\ (Y - y(x))\text{^}2]$ (5)

where n is the number of data points. The lower the MSE, the better the fit of the equation to the given data. The R-squared value was computed by subtracting the residual sum of squares (RSS) from the total sum of squares (TSS) and dividing by the TSS.

A python code that fits the logistic model to transmittance (P/Po) vs N_{Na} for NaB-CaB suspensions output values of the logistic model parameters a, b, c, and d besides RMSE and R^2 values and a plot of P/Po versus N_{Na} (Fig. 1a). A similar code used for fitting the logistic model to absorbance versus N_{Na} (Fig. 1b). The same for the KB-CaB case.

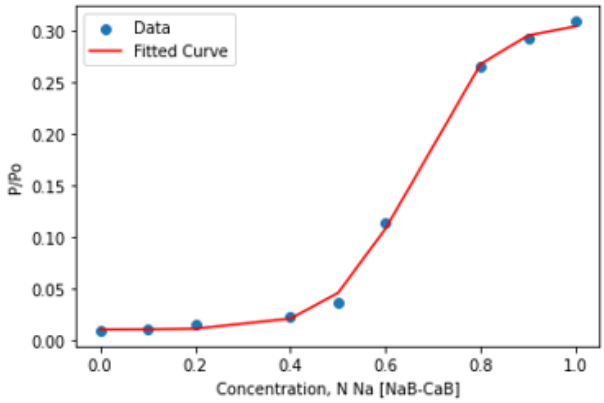

Optimized Parameters:
a = 0.3078744442222835
b = 0.6554818808442633
c = 12.855529887990219
d = 0.010515555945501368
Mean Squared Error (MSE):
2.050546223837511e-05
R-squared (R2): 0.9986617595213942
Fig. 1a

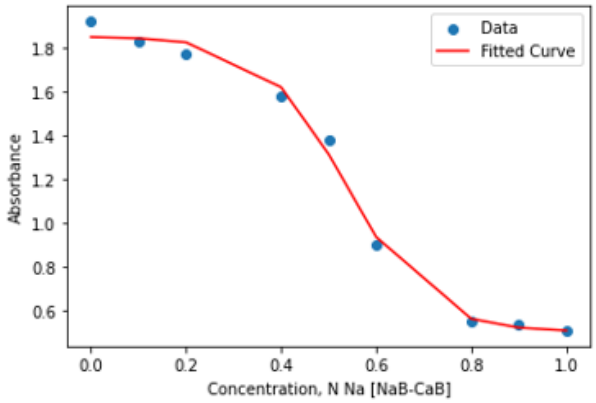

Optimized Parameters:
a = 0.5019079534046353
b = 0.5354772879051352
c = 11.6012946214472
d = 1.8500844119782578
Mean Squared Error (MSE):
0.0016671869997847883
R-squared (R2): 0.9947083238348302
Fig. 1b

Fig. (1): Output a Python code for fitting the logistic function to the spectrophotometer's transmittance, P/Po (Fig. 1a) and absorbance (Fig. 1b) versus N_{Na} for the NaB-CaB suspensions.

MATERIALS AND METHODS

MATERIALS

Used in this study a Na-bentonite < 75 µm clay sample (powder) supplied by the Sphinx Milling Station Company (Alexandria, Egypt) together with a Wyoming montmorillonite sample. The bentonite sediment was from Wadi El-natron valley (30° 26' 3.54" N, 30° 17' 6.90" E), Egypt. The bentonite sediment is processed by crushing, activation using 3-4% soda ash (Na_2CO_3), and watering, drying, and milling for a particle diameter of < 75 µm (200 mesh). We used in this study ELGA US ultrapure water (resistivity 18.2 MΩ), grade pure chemicals, and new optically matched silicate glass cuvettes from Starna, Germany.

METHODS

Preparing Nano Na-Bentonite Suspension

The Kokusan centrifuge H 100BC, Japan used in this study. Each centrifuge tube contained 1.50 g < 75 µm Na-bentonite in 20 ml deionized water (75 mg/ml) and rigorously suspended. The distance from the suspension's meniscus to the bottom of the centrifuge tube was 5.7 cm, and the distance from the center of the centrifuge's head to the suspension's meniscus at time 0 was 9.8 cm. The suspension was centrifuged at 5000 rpm (4332 × g) for 10 minutes. According to Barshad (1969) and Elprince (2015), the bentonite's impurities moved to the bottom of the centrifuge tube. After discarding the supernatant (invisible particles), the suspension above the impurities separated using a syringe, agitated, and centrifuged at 5000 rpm for 60 minutes. After removing the 3.0 cm supernatant (invisible particles) the 2.0 cm suspension down to a distance 0.25 cm above the bottom was separated using a syringe and collected into a container labeled (Susp a) for later use. Using Svedberg's equation (Svedberg and Nichols, 1923; Elprince et al., 2015) with η_L = 0.021 Pa s, ρ_L = 1 x 10^3 kg m^{-3}, and ρ_p = 2.2 x 10^3 kg m^{-3} the particle diameter D_i value was computed. This nano Na-bentonite (Susp a) had D_i values of 99 nm to 124 nm and its measured concentration and pH were 31.0 mg/ml and 8.81, respectively. This suspension was X-rayed, and TEM imaged.

Preparing Nano NaB, KB, and CaB Suspensions

A NaB suspension was prepared by leaching (centrifuging) the (Susp a) with 0.5 mole L^{-1} NaCl three times followed by deionized water until made chloride-free (tested negative with AgNO3). The concentration of this NaB suspension was determined by drying a sample at 105 C to a constant mass. Subsequently, the NaB suspension was diluted with deionized water to have a concentration equal to 14.4 mg NaB/ml suspension. Similar steps were followed using (Susp a), 0.5 mole L^{-1} KCl and 0.5 mol_c L^{-1} $CaCl_2$ to end with nano KB suspension and nano CaB suspension had a concentration equal to 12.5 mg KB/ml suspension and 13.4 mg CaB /ml suspension, respectively.

Preparing Nano NaB-CaB Mixtures

Computed volumes of the nano NaB suspension: 0.00, 1.74, 3.47, 6.94, 8.68, 10.41, 13.88, 15.62 and 17.36 ml were added to nine volumetric 50 ml flasks and completed to the mark using deionized water (Fig. 2). Computed volumes of the CaB suspension: 0.00, 1.74, 3.47, 6.94, 8.68, 10.41, 13.88, 15.62 and 17.36 ml were added to nine volumetric 50 ml flasks and completed to the mark using deionized water (Fig. 2). Mixing the two sets of volumetric flasks, pairwise in polyacrylic bottles (Fig. 2) yield salt-free Na-CaB suspensions having charge fractions of exchangeable sodium N_{Na} equal to 0.1, 0.2, 0.4, 0.5, 0.6, 0.8, and 0.9 while N_{Ca} equal to 1- N_{Na}. The corresponding NaB component concentrations (g $_{NaB}$ / 100 ml $_{suspn}$) were 0.025, 0.050, 0.100, 0.125, 0.150, 0.200, and 0.225. The corresponding CaB component concentrations (g_{CaB} / 100 ml $_{suspn}$) were 0.025, 0.050, 0.100, 0.125, 0.150, 0.200, and 0.225. The solid concentration in all the NaB-CaB suspensions was a constant equal to 2.5 mg_{solid} / ml_{suspn}.

Preparing Nano KB-CaB Mixtures

Following the same procedure of the preparation of the NaB-CaB suspensions a set of KB-CaB bottles were prepared. Computed volumes of the nano KB suspension: 2.00, 3.99, 7.99, 9.98, 11.98, 15.97, and 17.97 ml were added to seven volumetric 50 ml flasks and completed to the mark using deionized water. Similarly, computed volumes of the nano CaB suspension: 16.79, 14.93, 11.20, 9.33, 7.46, 3.73, and 1.87 ml were added to another seven volumetric 50 ml flasks and completed to the mark using deionized water. Mixing the two sets of volumetric flasks, pairwise in polyacrylic bottles yields KB-CaB suspensions free of salt having charge fractions of exchangeable potassium N_K equal to 0.1, 0.2, 0.4, 0.5, 0.6, 0.8, and 0.9 while N_{Ca} equal to 1 – N_K. The solid concentration in all the KB-CaB suspensions and the NaB-CaB suspensions was a constant equal to 2.5 mg_{solid} / ml_{suspn}.

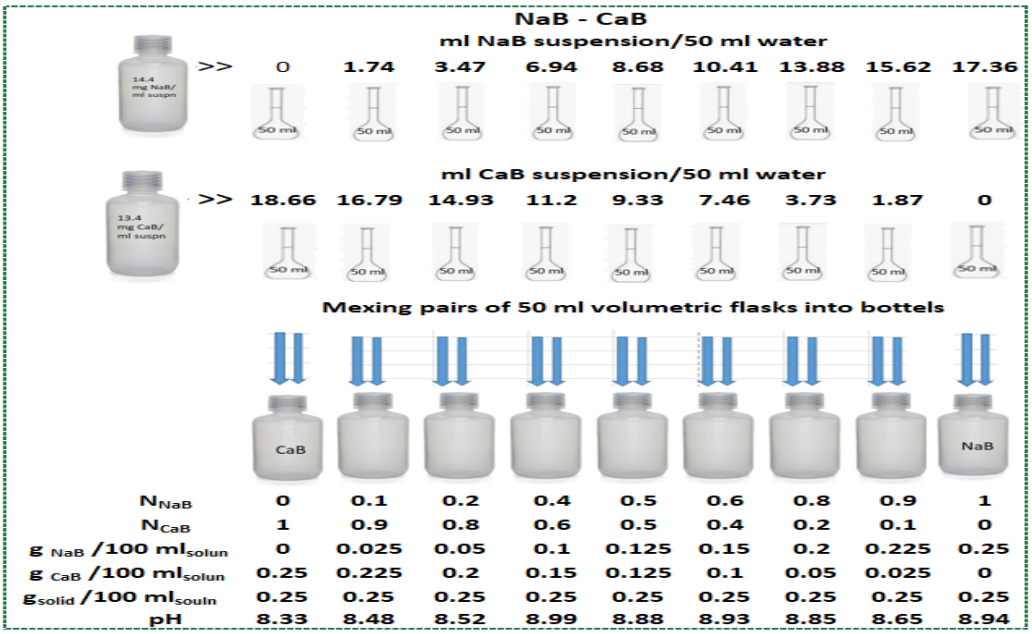

Fig. (2): Preparing NaB-CaB suspensions. N_{NaB} and N_{CaB} are charge fractions of exchangeable Na^+ and Ca^{2+} components of the nano bentonite<, respectively

X-ray Scattering

X-ray diffractograms (XRD) were done for nano Na-bentonite and Wyoming montmorillonite suspensions; each mounted on a glass slide, air dried giving an oriented sample. Both samples were x-rayed under the same instrumental conditions. The XRD was obtained with a Bruker Meas Srv (D2-208219)/D2-2082019 diffractometer, Germany, operating at 30 kV, 10 mA, and a Cu tube ((λ =1.54184 Å) with a $^o2\theta$ range of 0 to 100°. The X-ray diffractograms were processed using the software X'Pert HighScore Plus.

High Resolution Transmission Electron Microscopy

A transmission electron microscope (TEM) (JEOL, Model JSM 6360LA, Tokyo, Japan) was used in this study. The sample support was a Cu mesh grid, and the membrane support was carbon. A high-resolution TEM image was obtained for the nano Na-bentonite suspension.

RESULTS AND DISCUSSIONS

X-ray Results

As seen in Fig. 3 the XRD of Wyoming montmorillonite (blue) was superimposed on the nano Na-bentonite one (red). The smectite peaks S (001) and S (004) were most probably the montmorillonite peaks M (001) and M

(002) peaks. Montmorillonite is by far the most abundant smectite clay mineral in bentonites (Abdou et al., 2013; García-Romero et al., 2021). As seen in Fig. 3, two other clay minerals were identified in Nano Na-bentonite, namely kaolinite and illite (Moore and Reynold, 1989).

TEM Results

The presence of a fourth clay mineral, the palygorskite in the nano Na-bentonite was detected by TEM imaging (Bneotry, 1940). Palygorskite is a fibrous clay difficult to detect in X-ray patterns of an oriented sample (Moore and Reynolds, 1989). Palygorskite is made of laths grouped in a crystallographic arrangement, sharing edges or faces forming rods parallel to the c-axis of the fiber (Fig. 4).

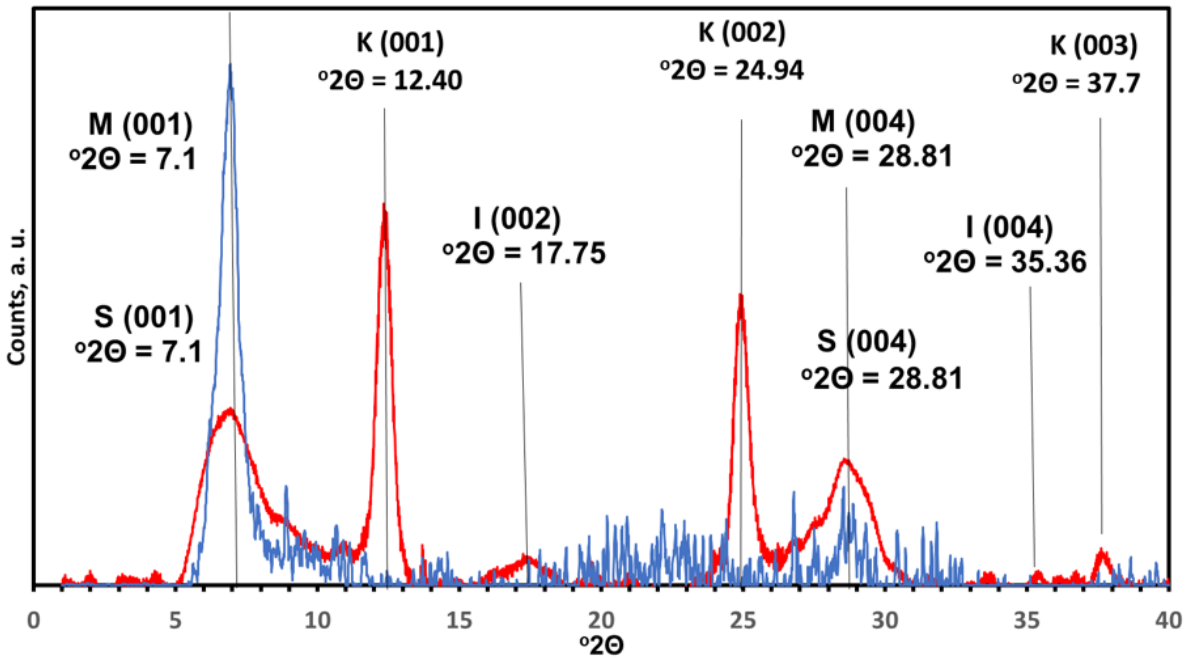

Fig. (3): Diffraction patterns of nano Na-bentonite (red) and Na-Wyoming montmorillonite (blue). The smectite type in the nano Na-bentonite is most probably a Na-montmorillonite.

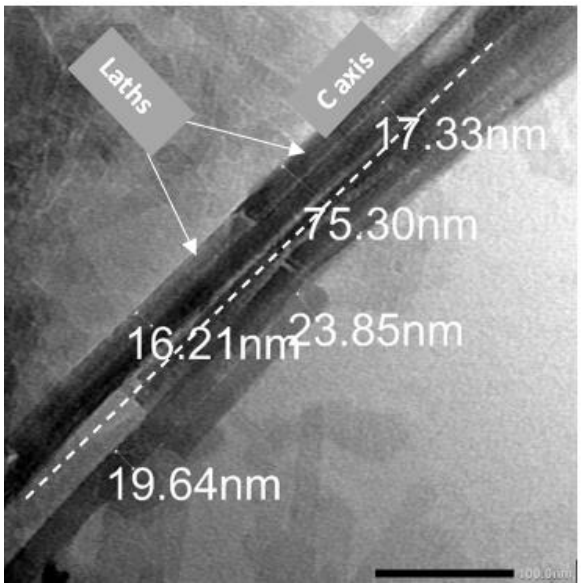

Fig. (4): TEM image for palygorskite in nano Na-bentonite. The scale is 10 nm.

As seen in Fig. 4 the laths (width 16-24 nm) are grouped in a crystallographic arrangement, sharing edges or faces forming rods. Several rods, parallel to the c-axis of the fiber, form bundles.

The Breakdown of Nano Ca Bentonite Tactoids by Exchangeable Na^+ and K^+

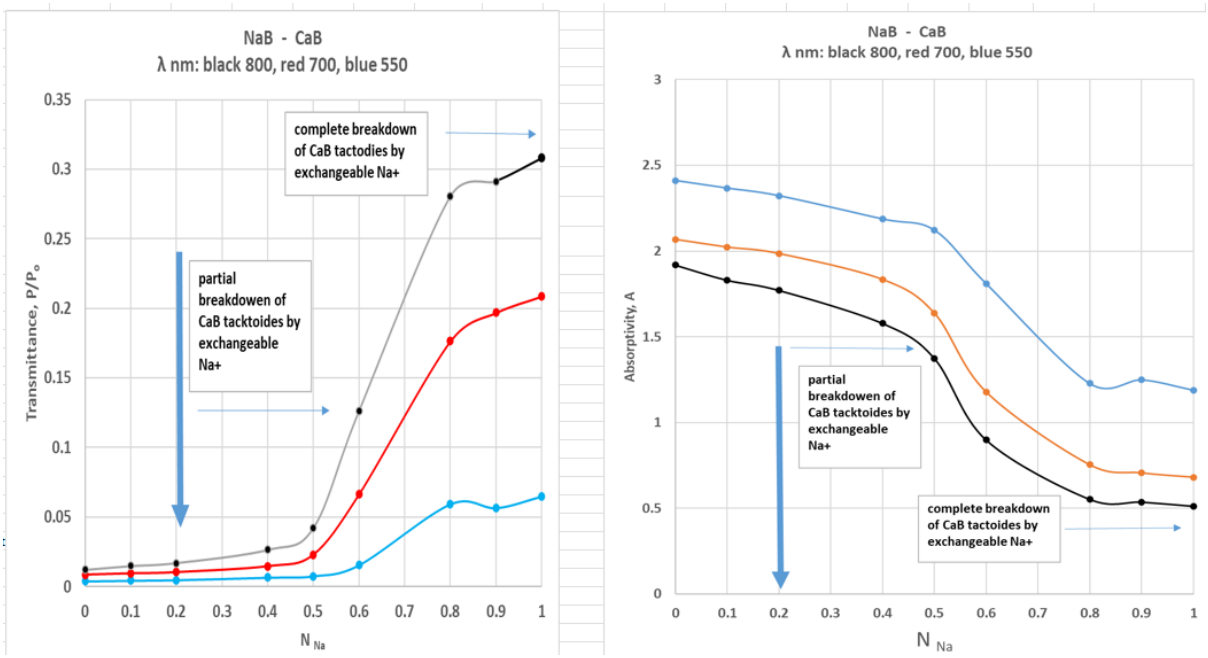

Fig. (5): The dependence of light transmittance (left figure) and absorbance (right figure) of nano Na-Ca bentonite suspensions (aged for 7 days after preparation) on the charge fraction of exchangeable Na^+ for three light wavelengths.

Figure 5 shows the dependence of light transmittance and absorbance by nano NaB-CaB suspensions (aged for 7 days after preparation) on the charge fraction of exchangeable Na^+ for the three wavelengths 800, 700, and 550 nm. These results indicated that the bentonite particles, specifically smectite tactoids, saturated with Ca^{2+} were subject to partial breakdown by exchangeable Na^+ up to N_{Na} equal to 0.5 (i.e., 50% exchangeable Na^+) followed by a steeper curve in case the wavelength, λ is 800 nm and a more gradual curve for λ equal to 700 and 550 nm. A complete breakdown of the Ca tactoids occurred for $N_{Na} > 0.8$.

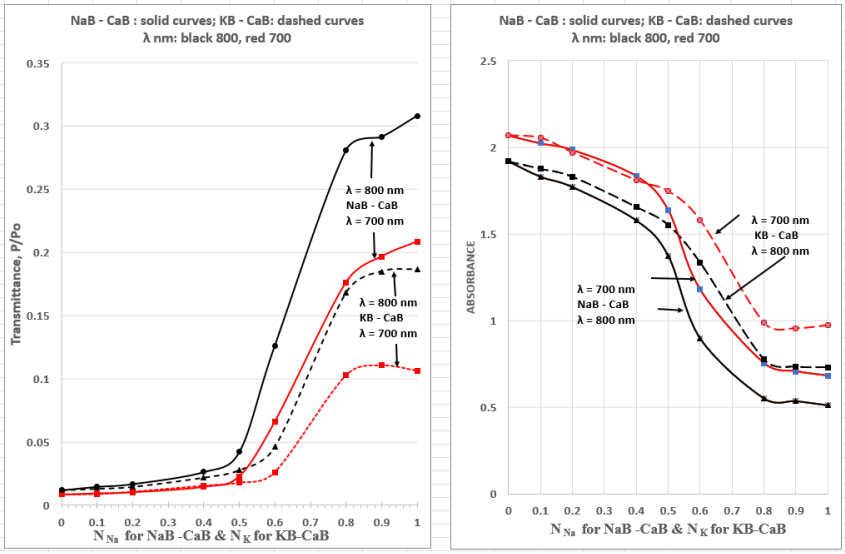

Fig. (6): Left figure: The dependence of light transmittance of nano NaB-CaB suspensions (solid curves) and nano KB-CaB suspensions (dashed curves) on the charge fraction of exchangeable Na^+ and exchangeable K^+, respectively; for the two wavelengths 700 nm (red) and 800 nm (black). These measurements were taken for suspensions aged for 7 days. Right figure: same as left figure but using the light absorbance instead of the transmittance

Figure 6 shows the dependence of light transmittance (lift figure) and absorbance (right figure) of both nano KB-CaB and NaB-CaB suspensions (aged for 7 days after preparation) on the charge fraction of exchangeable K^+ and Na^+, respectively for the two wavelengths 700, and 800 nm. These results indicated that the bentonite particles, specifically smectite tactoids, saturated with Ca^{2+} were subject to partial breakdown (delamination) by exchangeable Na^+ up to N_{Na} equal to 0.5 (i.e., 50% exchangeable Na^+) followed by a steeper curve in case the wavelength, λ is 800 nm and a more gradual curve for λ equal to 700 nm. A complete breakdown of the Ca tactoids to single Na-platelets occurred for $N_{Na} > 0.8$. Based on visualization by Montecarlo Simulation, Na^+ is bound in an outer-sphere surface complex on the siloxane surface of the Na-platelet of montmorillonite (Sposito et al., 1999).

On the other hand, for $0 < N_K < 0.5$, exchangeable K^+ was a staking agent due to fixation in the silicate's cavities. Based on visualization by Montecarlo Simulation, K^+ is bound in an inner-sphere surface in the interlayer region of montmorillonite (Sposito et al., 1999). For $0.5 < N_K < 0.8$, K^+ was a more effective ion exchanger (hydrated radius = 0 .331 nm) compared to Na^+ (hydrated radius = 0 .358 nm) for the replacement of exchangeable Ca (hydrated radius = 0 .412 nm). The magnitude of the standard free energy of replacing exchangeable Ca by K^+ expected to be greater than that of replacing exchangeable Ca by Na^+ (Gast, 1969). The values of the hydrated radii are from Danial et al. (2020; page 35) indicating sodium ion is structure making ion in water and potassium ion is structure breaking ion in water. As N_{K+} increased, the delamination of ca-tactoids occurred but with a rate of K-platelets growth lower than the rate of Na-platelets production by Na^+.

Fitting the absorbance data of (Fig. 6 right figure) to the logistic function (Eq. 3) gave the model parameters a, b, c, and d reported in Table 1

Table 1. Logistic function parameters for the absorbance curves (Fig. 4. right figure).

Reaction time 7 days after suspensions preparation.

Suspension	λ, nm	a	b	c	d	RMSE	R^2
NaB - CaB	700	0.679	0.562	12.2	2.030	0.0006	0.998
	800	0.502	0.535	11.6	1.850	0.0017	0.995
KB-CaB	700	0.885	0.619	9.2	2.029	0.0029	0.986
	800	0.653	0.606	8.9	1.883	0.0015	0.993

As seen in Table 1, while the c parameter values for KB-CaB suspensions were 9.2 and 8.9 for 700 nm and 800 nm wavelengths, respectively; the corresponding values for NaB-CaB suspensions were 12.2 and 11.6. The higher the c value the higher the growth production of the single platelets. As N_{Na+} increased, the delamination of ca- tactoids occurred with a rate of Na-platelets growth higher than the rate of K-platelets production by K^+.

The Ageing of Tactoids

To study the impact of aging on tactoid dynamics spectrophotometric absorbance data was measured for the nano NaB-CaB and KB-CaB suspensions after 7, 61, and 93 days of preparation at 800 nm light wavelength. The logistic function fitted to the absorbance data and the resulting a, b, c, and d model parameter values together with RMS and R^2 values are given in Table 2. According to the logistic model, the c value represented the single platelet's growth rate. As seen in Table 2 for the 7, 61, and 93 ageing days the c values were 11.6, 10.5, and 10.3 for the NaB-CaB suspensions and 8.9, 7.8, and 7.54 for KB-CaB, respectively. This result indicated that exchangeable Na^+ was, on average, a 34% more effective Ca-tactoid breaker than exchangeable K^+. Furthermore, a plot of the c values against the aging time (Fig. 7) indicated that the logistic parameter c values decreased and then leveled for both the NaB-CaB and KB-CaB suspensions indicating equilibrium after the 93 aging days.

Table 2. The effect of ageing days of suspensions on spectrophotometry light absorbance of nano NaB-Cab and KB-CaB suspensions at wavelength 800 nm fitted to a logistic function (Eq. 3) the parameters of which are a, b, c, and d.

Suspension	Ageing days	a	b	c	d	RMSE	R^2
NaB-CaB	7	0.502	0.535	11.6	1.850	0.0017	0.995
NaB-CaB	62	0.494	0.537	10.5	1.952	0.0023	0.993
NaB-CaB	93	0.485	0.5341	10.3	2.006	0.0024	0.994
KB-CaB	7	0.653	0.606	8.9	1.883	0.0015	0.993
KB-CaB	62	0.631	0.583	7.8	2.001	0.0023	0.991
KB-CaB	93	0.635	0.5487	7.54	2.069	0.0026	0.991

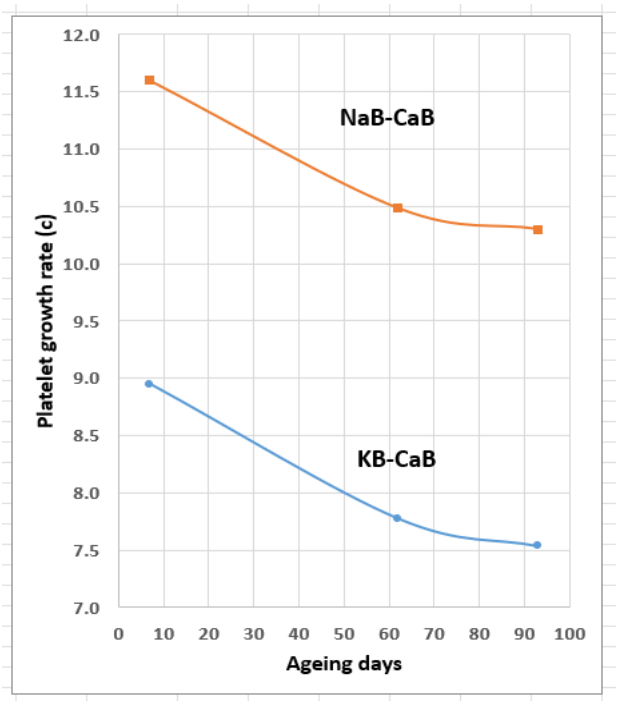

Fig. (7): The logistic function parameter c (single platelet's growth rate) values against ageing days for suspensions of NaB-Cab and KB-CaB.

The present study demonstrates that spectrophotometry with sound theoretical bases, carefully prepared suspensions, and logistic modelling, was a useful technique to characterize clay dispersion, particularly in aggregated systems.

ACKNOWLEDGMENTS

The authors wish to extend many thanks to Chemist Mohamed Morsy Tolba, Chairman of Sphinx Milling Station, Alexandria, Egypt, for providing both the Na-bentonite sample < 75 μm (powder) and a set of new optically matched silicate glass cuvettes from Starna, Germany.

References

Abdou, M. I., Al-Sabagh, A., and Dardir, M. (2013). Evaluation of Egyptian bentonite and nano-bentonite as drilling mud. *Egyptian Journal of Petroleum*, *22*(1), 53-59.

Aylmore, L., and Quirk, J. (1959). Swelling of clay–water systems. *Nature*, *183*(4677), 1752-1753.

Banin, A., and Lahav, N. (1968). Optical study of particle size of montmorillonite with various adsorbed cations. *Nature*, *217*(5134), 1146-1147.

Barshad, I. (1960). Significance of the presence of exchangeable magnesium ions in acidified clays. *Science*, *131*(3405), 988-990.

Birdi, K. (2008). *Handbook of surface and colloid chemistry*: CRC press.

Bneotrv, W. F. (1940). The structural scheme of attapulgite. *Amer. MineraL.*,25,405-470.

Brindley, G. (1980). Quantitative X-ray mineral analysis of clays.

Danial, G.S., Bohn, H.L, O'Connor, G.A. (2020). Soil Chemistry. 5th ed. Willey & Sons – Blackwell.

Elprince, A., Saffan, M., and Zabidi, M. (2015). Observed-Predicted Shifts in Thermodynamic Functions of Water Adsorption by Smectite at Nanoscale. *Soil Science Society of America Journal*, *79*(5), 1319-1328.

Enrique Macia'-Barber. (2020). Quazicrystals Fundamentals and applications. CRC Press. Taylor & Francis.

García-Romero, E., Lorenzo, A., García-Vicente, A., Morales, J., García-Rivas, J., and Suárez, M. (2021). On the structural formula of smectites: a review and new data on the influence of exchangeable cations. *Journal of Applied Crystallography*, *54*(1), 251-262.

Gast, R. (1969). Standard free energies of exchange for alkali metal cations on Wyoming bentonite. *Soil Science Society of America Journal*, *33*(1), 37-41.

Gieseking, J. E. (2012). *Soil Components: Vol. 2: Inorganic Components*: Springer Science & Business Media.

Keren, R., and Klein, E. (1995). Sodium/Calcium-Montmorillonite Suspension and Light Scattering. *Soil Science Society of America Journal, 59*(4), 1032-1035.

Kittel, C. (1953). *solid state physics*: John Wiley & sons, inc.

Mering, j. (1975). Smectites. In Gieseking, J. E. (Ed.) Soil Components. Vol. 2. Inorganic Components. Springer – Verlag, New York.

McEwen, M. B., and Pratt, M. I. (1957). The gelation of montmorillonite. Part 1.—The formation of a structural framework in sols of Wyoming bentonite. *Transactions of the Faraday Society, 53*, 535-547.

Maciá-Barber, E. (2020). *Quasicrystals: fundamentals and applications*: CRC Press.

Moore, D. M., and Reynolds Jr, R. C. (1989). *X-ray Diffraction and the Identification and Analysis of Clay Minerals*: Oxford University Press (OUP).

Shainberg, I., and Kaiserman, A. (1969). Kinetics of the formation and breakdown of Ca-montmorillonite tactoids. *Soil Science Society of America Journal, 33*(4), 547-551.

Shainberg, I., and Otoh, H. (1968). Size and shape of montmorillonite particles saturated with Na/Ca ions (inferred from viscosity and optical measurements). *Israel Journal of Chemistry, 6*(3), 251-259.

Sorensen, C.M. (2003). Scattering and absorption of Light by particles and aggregates. In: Birdi, K.S. (Ed) Handbook of surface and colloid chemistry, second edition. CRC Press LLC.

Sposito, G. (1984). The Surface Chemistry of Soils. Oxford University Press New York.

Sposito, G., Skipper, N. T., Sutton, R., Park, S. and Soper, A. K. (1999). Surface geochemistry of the clay minerals. Prov. Natl. Acad. Sci. USA. 96, 3358-3364.

Strawn, D. G., Bohn, H. L., and O'Connor, G. A. (2020). *Soil Chemistry*: Wiley.

Svedberg, T. and Nichols, J. B. (1923). Determination of size and distribution of size of particle by centrifugal method. Contribution from the laboratory of physical chemistry of the University of Wisconsin. Vol.45. 2910-2917.

Waseda, Y., Matsubara, E., and Shinoda, K. (2011). X-ray diffraction crystallography: introduction, examples and solved problems: Springer Science & Business Media.

الملخص العربى

التحليل الطيفي الضوئي لتكسر تاكتويدات الكالسيوم النانونية بواسطة كاتيونات الصوديوم والبوتاسيوم القابل للتبادل الأيوني

أحمد رضا محمد غنيمي راغب محمد العادلي عادل محمد البرنس

قسم الأراضي والكيمياء الزراعية – كلية الزراعة سابا باشا – جامعة الإسكندرية

يشكل معدن المنتموريللونيت الموجود عادتا في الجزء الطيني بالأراضي تاكتويدات الكالسيوم التي تتكون من صفيحات متراصة رأسيا. من خلال عمليات التبادل الأيوني يمكن أن تؤدي التفاعلات بين الكاتيونات الموجودة في محلول التربة، مثل الصوديوم والبوتاسيوم لتفكك هذه الهياكل إلى صفيحات مفردة، وبالتالي التأثير على خصائص التربة. وقد استخدمت الدراسات السابقة القياس الطيفي لقياس خصائص معلقات المنتموريللونيت حيث تم دراسة ظواهر مثل انتقال الضوء وتشتته. ومع ذلك، توجد تحديات في تطبيق هذه الطرق بدقة، لاسيما فيما يتعلق بالإختلافات في تركيبة الأيونات المدمصة ونطاق حجم الحبيبات. تهدف هذه الدراسة إلي معالجة هذه التحديات وتعزيز الفهم من خلال 1- تطوير إطار نظرى للقياس الطيفي الذى يعزز الحساسية لأبعاد الجسيمات 2- تحليل ثوابت الدالة اللوجستية لإكتساب رؤى حول نمو الصفائح الفردية 3- التحقيق في آثار تقادم المعلق علي تكتل التاكتويدات. أشارت نتائج التصوير بالميكروسكوب الإلكتروني ومنحنيات أشعة إكس إلي أن نانو بنتونيت الصوديوم بعد إزالة الشوائب من العينة إحتوت علي أربعة معادن طين وهي السمكتايت (على الأرجح منتموريللونيت)، والكاؤلينيت، والإليت، والباليغوريسكت .أستخدم هذا النانو بنتونيت الصوديوم لتحضير معلقات نانو NaB–CaB خالية من الأملاح والتى تحتوى على أجزاء من شحنة من الصوديوم القابل للتبادل الأيونى، تساوى 0.0, 0.1, 0.2, 0.4, 0.5, 0.6, 0.8, 0.9, 1.0. تم إعداد مجموعة مماثله لمعلقات النانو KB–CaB. أظهرت النتائج أن تاكتويدات السمكتيت المشبعة بـ Ca+2 تخضع لتكسير جزئى بواسطة Na+ المتبادل حتى الجزء من الصوديوم القابل للتبادل الأيونى يساوى 0.5 ، لينتج زيادة أكثرإرتفاعا في نفاذية الضوء وإنخفاضا في الامتصاص عند الطول الموجي 800 nm مقارنة بـ 700 و550. وقد حدث الإنهيار الكامل لتاكتويدات Ca عندما الجزء لشحنة الصوديوم أصبح فوق 0.8. وعلى العكس من ذلك فإن K+ المتبادل يعمل كعامل تراصٍ حتي جزء الشحنة من البوتاسيوم يساوى 0.5 مما يؤدى إلى تباطؤ نمو الصفائح الفردية مقارنة بـ Na+. كشفت عمليات محاكاة مونت كارلو عن سلوك ارتباط متميز لأيونات Na+وk+ على سطح البنتونيت. وعلاوة على ذلك سلطت الدراسة الضوء على الفاعلية الأعلى لـ K+ بالمقارنة بـ Na+ لإستبدال Ca+2 إلى الإختلافات فى أنصاف أقطار الأيونات المتأدرتة وقيم الطاقة الحرة القياسية. وبشكل عام، ساهمت هذه النتائج فى فهم أعمق لديناميكيات التفكك فى معلقات NaB–CaB وKB–CaB النانوية على مدار 7 و61 و93 يوما. كشفت بيانات قياس الطيف الضوئي، التي تم قياسها عند الطول الموجي 800 nm عن وجود اختلافات واضحة في معدلات نمو الصفيحة المفردة (معامل الدالة اللوجستية c) بين معلق NaB–CaBومعلق KB–CaB وعلي وجه التحديد، كان NaB–CaB ذو قيم لـ cأعلى على مدار جميع فترات التقادم، وعلى وجه التحديد، كان Na+ المتبادل 34% أكثر فاعلية من K+ المتبادل في تكسير تاكتويدات الكالسيوم. توضح الدراسة الحالية أن القياس الطيفى الضوئى مع النظرية السليمة، والمعلقات المعدة بعناية، والنمذجة اللوجستية كانت تقنية مفيدة لتوصيف تشتت الطين، خاصة في الأنظمة المجمعة.